[CANCER RESEARCH 61, 532–537, January 15, 2001]

Direct Evidence of the Importance of Stromal Urokinase Plasminogen Activator (uPA) in the Growth of an Experimental Human Breast Cancer Using a Combined *uPA* Gene-Disrupted and Immunodeficient Xenograft Model

Thomas Leth Frandsen, Claus Holst-Hansen, Boye Schnack Nielsen, Ib Jarle Christensen, Jens R. Nyengaard, Peter Carmeliet, and Nils Brünner[1]

The Finsen Laboratory, Copenhagen University Hospital, DK-2100 Copenhagen, Denmark [T. L. F., C. H-H., B. S. N., I. J. C., N. B.]; Stereological Research Laboratory, Bartholin Bygningen, Aarhus University, 8000 Århus C, Denmark [J. R. N.]; and Center for Transgene Technology and Gene Therapy, Flanders Interuniversity Institute for Biotechnology, University of Leuven, B-3000 Leuven, Belgium [P. C.]

ABSTRACT

Several studies have indicated an interaction between tumor cells and infiltrating stromal cells regarding the urokinase plasminogen activation (uPA) system. By developing combined *uPA* gene-disrupted and immunodeficient mice, we have studied the role of stromal uPA for the growth of the MDA-MB-435 BAG human tumor xenograft. Subcutaneous tumor growth and lung metastasis were compared between wild-type immunodeficient mice and mice with the combined deficiencies. Tumor growth was evaluated by volume measurements and plasma β-galactosidase activity and metastasis was evaluated by counting lung surface metastases. Although no differences appeared in primary tumor take between the two groups of mice, a significant difference was observed in primary tumor growth, with tumors in uPA$^{-/-}$ mice growing significantly more slowly. In addition, a nonsignificant trend toward fewer lung metastases in uPA$^{-/-}$ mice was observed. The present data points to a critical role of stromal-derived uPA in the primary tumor growth of MDA-MB-435 BAG xenografts, whereas only a trend toward fewer lung metastases in *uPA* gene-disrupted mice was found.

INTRODUCTION

Proteinases such as matrix metalloproteinases, serine proteinases, and cystein proteinases have been suggested to play a critical role in cancer progression, *i.e.*, tumor growth, invasion, and dissemination. In particular, the urokinase plasminogen activation system, constituting uPA,[2] its specific receptor, uPAR, and its inhibitors, PAI-1 and PAI-2 have in experimental *in vivo* tumor models been shown to be involved in these processes. uPA is secreted as an inactive single-chain proenzyme (pro-uPA), which is converted by limited proteolysis into the enzymatically active two-chain uPA, which in turn cleaves plasminogen, resulting in the formation of the broad spectrum proteolytic enzyme plasmin. Both pro-uPA and uPA bind with high affinity to a specific cell surface receptor, uPAR. Concomitant cell surface binding of uPA and plasminogen focalizes and enhances plasmin formation to the close vicinity of the cell surface. Formation of uPA-PAI-1 complexes on the cell surface leads to internalization of the uPAR-uPA-PAI-1 complexes.

In situ hybridization and immunohistochemistry studies of human breast cancer tissue have shown that uPA mRNA and protein is mainly expressed by myofibroblasts surrounding nests of cancer cells (1), whereas uPAR is mainly expressed by infiltrating macrophages (2), suggesting that the stromal-cell components of the tumor tissue are actively involved in the expression of proteolytic activity. Whether these stromal cells represent a particular subpopulation of stromal cells that are recruited into the tumor tissue, or whether they are preexisting but induced by the tumor cells to produce proteinases, has not yet been not clarified. We have shown previously that in human breast tumors grown in immunodeficient mice, murine uPA is expressed by the mouse stromal cells with a pattern similar to that described in human breast cancer (3).

Experimental *in vitro* and *in vivo* studies have shown that inhibition of uPA activity or uPA-binding to uPAR results in tumor growth inhibition and reduced or abolished formation of metastasis (4–8). uPA is most probably facilitating cancer invasion by stimulating extracellular matrix degradation, but the exact role of uPA in regulating tumor growth is not fully understood. uPA may also be involved in activation of latent growth factors, *e.g.*, latent transforming growth factor β (9), and release of growth factors that are bound to the extracellular matrix, *e.g.*, basic fibroblast growth factor (10), and thereby regulate the growth of tumors by increasing the liberation and availability of these growth factors. In addition, uPA has been directly associated with cell proliferation, migration, and chemotaxis (11–16), all events that could have a significant impact on tumor cell dissemination.

Mice made genetically deficient for *uPA* show only minor phenotypic changes, such as occasional fibrin deposition in the intestines and in the sinusoids of the liver (17). *uPA*-deficient mice have, in addition, been shown to have impaired neointima formation after electric or mechanical injury of arteries, possibly attributable to an impaired cellular migration of smooth muscle cells (18–20), and a recent study showed that during the first 3 days of life, the epidermis from *uPA* gene-deficient mice have a significantly lower proliferative rate than the epidermis from wild-type mice, suggesting a role of *uPA* in epidermal cell proliferation (15). In accordance, wound-healing experiments have shown delayed healing in *uPA* gene-deficient mice (21). In another study, chemical induction of melanocytic neoplasms in mice revealed that wild-type and *uPA* gene-deficient mice developed blue nevi with the same frequency, whereas only wild-type mice had the ability to develop melanomas, suggesting a critical role of *uPA* in the final progression toward the fully developed malignant phenotype (22).

In the present study, we have established combined *uPA* gene-disrupted and immunodeficient mice. By transplanting a human cell line expressing only small amounts of human uPA into these mice and their wild-type littermates, we have tested the hypothesis that stromal uPA plays an important role in the growth and dissemination of this xenograft tumor model. The results support a direct role of stromal uPA in the growth regulation of the MDA-MB-435 BAG xenograft, whereas only a trend toward fewer metastasis in *uPA* gene-disrupted mice was found.

MATERIALS AND METHODS

Animals. Mice were kept in micro-isolation cages and fed a regular chow. The generation of *uPA*$^{-/-}$ mice has been described previously (17). The *uPA*

Received 6/26/00; accepted 11/13/00.

The costs of publication of this article were defrayed in part by the payment of page charges. This article must therefore be hereby marked *advertisement* in accordance with 18 U.S.C. Section 1734 solely to indicate this fact.

[1] To whom requests for reprints should be addressed, at The Finsen Laboratory, Copenhagen University Hospital, Strandboulevarden 49, Boulevard 86.2, DK-2100 Copenhagen, Denmark. Phone: 45-35455606; Fax: 45-35251117; E-mail: nils@finsenlab.dk.

[2] The abbreviations used are: uPA, urokinase plasminogen activator; uPAR, uPA-specific receptor; PAI-1 and PAI-2, plasminogen activator inhibitors type 1 and 2; pro-uPA, uPA pro-enzyme; β-gal, β-galactosidase.

gene-targeted mice of a mixed C57Bl6J/129 background were backcrossed 5 generations into the META/Bom substrain of BALB/c background (Bomholtgaard, Ry, Denmark). Littermate offspring were made by mating a $uPA^{+/-}$ META/Bom nu/nu male with a $uPA^{+/-}$ female of the META/Bom nu/+ genotype. In all experiments involving wild-type mice as controls, these were littermates to the *uPA*-deficient mice. All mice used for experiments were between 8–12 weeks old at the start of the experiment. All experimental evaluations were performed by an investigator unaware of animal genotype. For the initial characterization of *uPA* mRNA expression and protein production, the three included human breast cancer cell lines (see below), were grown in female META/Bom nu/nu mice. All animal experiments were performed according to the guidelines published by the Danish Animal Care Committee (permission no. 1998/561-146).

Genotyping was performed by standard procedure PCR analysis of tail DNA specimens. Genotyping of the animals was performed before and after experiments. The following primers were used: (*a*) Neo, 5′ ATG ATT GAA CAA GAT GGA TTG CAC G 3′; 5′ TTC GTC CAG ATC ATC CTG ATC GAC 3′; and (*b*) uPA, 5′ CTG GAA TGC GCC TGC TGT CCT TCA 3′, and TGT CAC GAG CTG CCC TGG GAA TCA 3′.

Cell Lines. Human breast cancer cell lines MDA-MB-435 BAG, MDA-MB-231 BAG, and MCF-7 BAG, which have been transduced with a replication-defective Moloney murine leukemia retroviral vector (M-MuLV) containing both *neoR* (neomycin resistance) and *lacZ* genes (23), were routinely propagated in Eagle's MEM with Glutamax-1 and supplemented with 5% FCS.

For the animal experiments, cells were harvested from subconfluent monolayer cultures by scraping with a rubber policeman. Cells were inoculated (2×10^6 cells/site) s.c. bilaterally into the abdominal flanks of the animals. Tumors were measured twice weekly in two dimensions with a caliper. Mice inoculated with MCF-7 BAG cells received a 0.72-mg Estradiol pellet (Innovative Research), at the time of cell inoculation. At the end of the experiments, the tumor-bearing mice, which were used for *in situ* hybridization and immunohistochemistry, were sacrificed by perfusion-fixation with PBS and 4% paraformaldehyde. The tumors were removed, bisected, fixed in 4% paraformaldehyde overnight and then paraffin-embedded. Tumors being used for ELISA and Northern blotting were snap-frozen in liquid nitrogen and stored at −80°C until analyzed. Lungs for metastasis evaluation were removed from mice that had been perfused with PBS.

***In Situ* Hybridization.** The probe to murine uPA, designated pMUPA07, is a 608-1642-bp cDNA fragment in pGEM5z, whereas the probe to human uPA, designated pHUPA13, is a 791-1303-bp cDNA fragment in pBluescript KS(+). Plasmids were linearized using the following restriction endonucleases: (*a*) pMUPA07, *Eco*RI or *Pst*I; (*b*) pHUPA13, *Hin*dIII. The probes obtained from these plasmids are specific for murine or human *uPA* mRNAs and do not cross-react (3). Generation of ^{35}S-UTP-labeled antisense and sense probes was performed by *in vitro* transcription of the plasmids using the relevant RNA polymerases (3). All probe preparations, including both sense and antisense probes, were adjusted to 1×10^6 cpm/μl (3). *In situ* hybridization was performed by the method of Kristensen *et al.* (24). Briefly, 5-μm tumor tissue sections cut from formalin-fixed, paraffin-embedded tissues were treated with proteinase K. After incubation overnight at 47°C with a hybridization solution containing radiolabeled RNA probe, the sections were washed twice in a 50% formamide solution for 1 h. The sections were then treated with RNase A, dehydrated, and air-dried. Autoradiographic emulsion was applied and sections developed 1 week after exposure.

ELISA for Human uPA. Human xenograft tumors were pulverized with a precooled powder pistol. The tissue powders were suspended at a ratio of 1:4 in extraction buffer [75 mM potassium acetate, 0.3 M NaCl, 0.1 M L-arginine, 10 mM EDTA, and 0.25% Triton X-100 (pH 4.2); Ref. 25] at 4°C. The suspensions were centrifuged at 105,000 × *g* for 1 h at 4°C, and the resulting supernatants were stored at −80°C.

Total human uPA concentrations in tumor extracts were measured using an ELISA kit from Oncogene Science (Cambridge, MA; Ref. 26). This assay uses two murine monoclonal antibodies to human uPA for catching and a rabbit polyclonal antibody to human uPA for detection. To test for species specificity, serial dilutions in duplicates of purified murine pro-uPA (a generous gift from Karin List, The Finsen Laboratory, Copenhagen, Denmark) starting from 2.0 ng/ml, then 1.0, 0.5, 0.25, 0.125, 0.0625 ng/ml, were assayed. Protein concentrations of the tissue extracts were determined using the Bio-Rad protein assay (Bio-Rad, Richmond, CA) with BSA as standard.

Northern Blotting. For Northern blots, 15 μg of total RNA derived from each tumor sample was size-fractionated by electrophoresis in 1.0% denaturating agarose gels containing formamide and transferred to reinforced nitrocellulose membranes. The cDNA probes used were pHUK8, carrying a 1.6kb *Pst*I fragment of a human uPA cDNA (27) and pHFβA-3′UT, coding for the 3′-untranslated region of human β-actin cDNA (28). The probes were labeled by the random priming method (29) using dc tp 5′-α-^{32}P triphosphate. Hybridization of blots was carried out at 42°C for 16 h in 50% formamide, 10 × Denhardt's solution, 0.5% SDS-5× SSC, 200 μg/ml salmon sperm DNA, 10% dextransulfate, 200 μg/ml yeast-tRNA, and 2×10^9 dpm/μg of ^{32}P-labeled probe. The filters were washed at 65°C for 1 h in 2× SSC-0.1% SDS, at 65°C for 1 h in 0.2× SSC-0.5% SDS, and at 65°C for one-half h in 0.1× SSC-0.5% SDS. Autoradiography was performed at −80°C using Kodak T-MAT-G films and Kodak Lanex x-omatic intensifying screens.

Quantitation of Lung Metastasis. Lung metastases were stained and counted essentially as described previously (23). Briefly, anesthetized animals were PBS-perfused, after which the lungs were dissected from the animals and placed in a mixture of 2% (v/v) paraformaldehyde and 0.2% (v/v) glutaraldehyde in PBS for 3–4 h at 4°C. After fixation, the tissue blocks were rinsed three times with PBS and then incubated for 24 h at 4°C in 1 mg X-gal/ml; 35 mmol/l potassium ferricyanide; 35 mmol/l potassium ferrocyanide; 2 mmol/l $MgCl_2$; 0.02% (v/v) NP40; and 0.01% (w/v) sodium deoxycholate in PBS. The lungs were then rinsed, first with 3% (v/v) dimethyl sulfate in PBS and then with PBS only. Until evaluation of surface metastases, the lungs were stored at 4°C in 0.02% sodium azide in PBS. Metastases were evaluated by counting surface metastases through an inverted dissecting microscope.

***β*-Gal Measurement in Plasma.** Blood was obtained from each mouse, and citrate plasma was separated. Plasma β-gal activity was measured by an immunocapture assay as described previously (30). Briefly, white microwell plates (Berthold, Bad Wildbad, Germany) were coated for 16 h at 4°C with 200 μl/well of the murine monoclonal antibody to *Escherichia coli* β-gal clone 5B88 (2.5 μg IgG/ml; Life Technologies, Inc., Gaithersburg, MD) in 0.1 M carbonate buffer (pH 9.5). Before use, the assay wells were rinsed once with 200 μl/well of SuperBlock solution (Pierce Chemicals, Rockford, IL) diluted 1:1 with PBS, and then by three washes with PBS containing 1 mg/ml Tween 20. Wells were then incubated for 1 h at 37°C with 200 μl/well in triplicate of 1:20 diluted plasma samples. After β-gal binding, the wells were washed three times with PBS containing 1 mg/ml Tween 20 and then treated for 45 min at 37°C with 200 μl/well of Galacto-Light Reaction Buffer Diluent with Galacton-Plus chemiluminescent substrate (Tropix, Bedford, MA). After the enzymatic cleavage of the substrate, chemiluminescent light emission was triggered by adding automatically 100 μl/well of the alkaline polymeric enhancer (Accelerator-II; Tropix) using the pump incorporated in the luminometer (Berthold LB 96 P-2 MicroLumat). Chemiluminescence intensity (relative light units) was measured over a 5-s interval with a delay time of 2 s. The results are presented as the mean ± SE.

CD34 Immunohistochemistry. Five-μm paraffin sections of the tumors were deparaffinized in xylene and hydrated through ethanol/water dilutions. Proteolytic digestion was performed with 0.025% trypsin (Sigma T8128) in 50 mM Tris (pH 7.6) containing 0.1% $CaCl_2$ for 7 min at 37°C. Sections were blocked for endogenous peroxidase activity by 1% hydrogen peroxide for 15 min. Then, sections were washed in TBS [50 mM Tris, 150 mM NaCl (pH 7.6)] containing 0.5% Triton X-100. Slides were mounted into Shandon sequenza slide racks with immunostaining cover plates (Shandon Inc. Pittsburgh, PA, USA), for additional incubations. The sections were incubated overnight at 4°C with rat antimouse CD34 (clone MEC 14.7, HyCult Biotechnology, Uden, Netherlands) at 1:30 (3 μg/ml). The rat antibody was detected with affinity purified biotinylated rabbit antirat antibodies (E468, Dako, Glostrup, Denmark) followed by streptavidin horseradish peroxidase complexes (Dako, Glostrup, Denmark). Each antibody incubation was followed by washes with 6 ml of Triton X-100. Sections were developed with NovaRED substrate as specified by the manufacturer (Vector Laboratories, Burlingname, CA) for 10 min. Finally, sections were counterstained in diluted Mayers Hematoxylin for 30 s, dehydrated in ethanol, and mounted.

Quantitation of Angiogenesis. The computer-assisted stereology setup consisted of a Leica Dialux 22 microscope equipped with a CCD Camera (JAI 2040) and a motorized X-Y stage directed by a multicontroller unit (Olympus, Albertslund, Denmark). The computer (IBM, PC 300 GL) had a 24-bit frame-

grabber board (Screen Machine, FAST SMII) and CAST-grid software (Olympus, Denmark) installed as described elsewhere.[3]

The vascular length density was estimated with an unbiased counting frame as described by Gundersen *et al.* (31), with the assumption that the vessels were isotropic in the tumor. Counting was performed on CD34 immunohistochemically stained sections (two from each tumor), which were slightly counterstained with hematoxylin. The overall magnification used on the computer monitor was ×318. The vascular length density [L_V(vasc/tumor)] estimates were obtained by counting vascular profiles [Q_A(vasc)] within the counting frame. The upper right corner was used to estimate the tumor tissue by point-counting [ΣP(tumor)]. The area associated to this test point was denoted (*a/p*). Only vital tumor areas and vascular profiles located within living tumor areas were counted. The vascular length density was estimated as:

$$L_V(\text{vasc/tumor}) = \frac{Q_A(\text{vasc})}{\{2 \cdot (2 \cdot \Sigma P(\text{tumor})\}}$$

The average radius of the living tumor around a "typical" capillary, which may be interpreted as the average maximal diffusion distance from capillary to tumor, $\bar{r}$ (tumor/vasc), was obtained by:

$$\bar{r}\ (\text{tumor/vasc}) = \{\pi \cdot L_V(\text{vasc/tumor})\}^{-1/2}$$

The total length of vessels in vital tumor tissue was obtained by

$$L(\text{vasc}) = L_V(\text{vasc/tumor}) \cdot V(\text{tumor})$$

.

Statistical Methods. For the comparison of primary tumor growth curves of the two groups, repeated measures of ANOVA were used. The statistical significance of differences in plasma β-gal activity, vascular length density, maximal diffusion distance, and total length of vessels were analyzed by Student's *t* test. The number of metastases formed in the two groups was compared by Fischer's exact test and the nonparametric Mann-Whitney test. In all statistical analyses, *P*s < 0.05 were considered statistically significant.

RESULTS

Expression of Human and Murine uPA mRNA and Human uPA Protein in Xenografted Tumors. To select a human breast cancer xenograft with low endogenous human-uPA expression, Northern blot analysis using a human-specific cDNA uPA probe (3) was performed on total RNA purified from primary tumor xenografts. MDA-MB-231 BAG cells expressed measurable levels of human uPA mRNA, whereas a total lack of signal was found in MDA-MB-435 BAG and MCF-7 BAG tumors (Fig. 1). Extracts from MDA-MB-231 BAG and MDA-MB-435 BAG tumors were investigated in a human-specific uPA ELISA, and in accordance with the Northern blot analysis, the ELISA measurement showed that whereas MDA-MB-231 BAG tumors express high amounts of human uPA (84 ng/mg protein ± SD), MDA-MB-435 BAG cells contained 400-fold less uPA/mg protein (0.22 ng/mg protein ±SD). By applying the ELISA to a standard curve of murine uPA, it was confirmed that this assay does not detect mouse pro-uPA (not shown). Thus, the uPA protein measured is exclusively produced by the human cancer cells.

Because the MDA-MB-435 BAG xenografts express a low level of human uPA mRNA and protein, and because MDA-MB-435 BAG xenografts, different from MCF-7 xenografts, are known to grow locally invasive and to form lung metastases (23), this xenograft was selected for additional experimentation.

***In Situ* Hybridization of Human and Murine uPA.** *In situ* hybridization of MDA-MB-435 BAG xenografts for human uPA using a species-specific RNA probe (3), showed a weak but homogenous

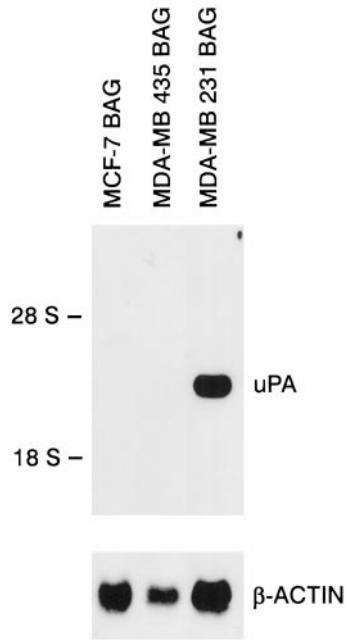

Fig. 1. Northern blot analysis of human uPA mRNA in extracts of MDA-MB-231 BAG, MDA-MB-435 BAG, and MCF-7 BAG tumor xenografts. Total RNA was electrophoresed in agarose gels under denaturating conditions and blotted onto a nitrocellulose membrane. The membrane was hybridized with a human cDNA probe for uPA. *Lane 1*, RNA from MCF-7 BAG tumors; *Lane 2*, RNA from MDA-MB-435 BAG tumors; and *Lane 3*, RNA from MDA-MB-231 BAG tumors. The lanes were loaded with 15 μg of total RNA. The *lower* section shows a control rehybridization of the membrane with a β-actin cDNA probe. The electrophoretic mobility of rRNAs is indicated to the *left*.

signal over the tumor cells, with no signal observed in the host stromal tissue (data not shown). No specific signal was obtained by the corresponding sense probe (data not shown). In contrast, when using the mouse-specific probe, distinct regions of murine uPA expression were apparent within the stromal cells of the tumors. Expression was predominantly seen at the stromal regions near the tumor periphery, usually in the areas of invasion (Fig. 2, *A* and *C*). Murine uPA mRNA was also strongly expressed in regions bordering the necrotic areas (Fig. 2, *B* and *D*). At higher magnification, murine uPA was found to be expressed by stromal cells near the tumor-stroma border, including some endothelial-like cells. Although some endothelial cells (or cells in the vicinity of endothelial cells) did appear to express murine uPA mRNA, the signal was generally not associated with vascular-appearing structures, suggesting nonendothelial stromal cells as the major expressors of murine uPA. No murine uPA mRNA signal was detected in tumors obtained from $uPA^{-/-}$ mice or when using the sense probe on tumors from wild-type mice (data not shown).

Formation of MDA-MB-435 BAG Tumors in $uPA^{+/+}$ Immunodeficient Mice and in Combined *uPA* Gene-Disrupted and Immunodeficient Mice ($uPA^{-/-}$). Three separate experiments were performed, including a total of 34 $uPA^{+/+}$ and 36 $uPA^{-/-}$ immunodeficient mice, each of which had bilateral tumor cell inoculation. In all three experiments, the mice were sacrificed about day 50, when tumors in the $uPA^{+/+}$ mice had reached a mean volume of approximately 2000 mm^3.

In the $uPA^{+/+}$ mice, 34 of 34 animals (100%) developed tumors in the experimental period. MDA-MB-435 BAG cells formed tumors in $uPA^{-/-}$ mice with the same frequency as in $uPA^{+/+}$ mice, suggesting that host (murine) uPA is not essential for MDA-MB-435 BAG tumor formation. No differences in length of lag phase (time to palpable tumors) was observed between tumors growing in the two mouse genotypes.

MDA-MB-435 BAG tumors in $uPA^{+/+}$ mice grew rapidly and

[3] Nielsen, B. S., Lund, L. R., Christensen, I. J., Johnsen, M., Autzen, P., Andersen, L. W., Frandsen, T. L., Danø, K., and Gundersen, H. J. A precise and efficient method to determine murine lung metastasis volumes using stereology, submitted for publication.

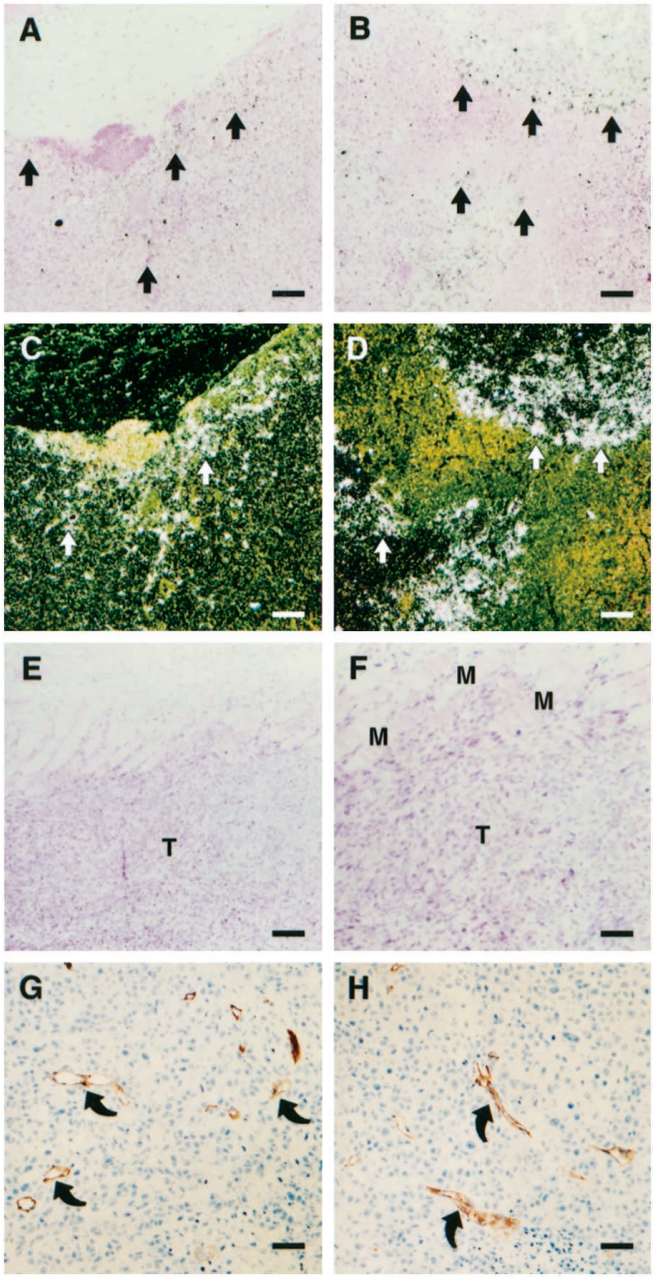

Fig. 2. Murine-uPA mRNA expression as determined by *in situ* hybridization on MDA-MB-435 BAG xenografted tumors grown in wild-type mice (*A*, *B*, *C*, and *D*). *A* and *C* demonstrate an area of invasion into musculus panniculus of the host. *B* and *D* show an area of necrosis and non-necrotic tumor tissue. *Arrows* show areas of murine uPA mRNA expression. *E* and *F* are HE stainings of an area in a MDA-MB-435 BAG xenografted tumor in a uPA−/− mouse. The cancer cells invade the abdominal muscle of the host. *T*, non-necrotic tumor tissue; *M*, peritoneal muscle tissue. *G* and *H* show CD34 immunostaining of the MDA-MB-435 BAG xenografted tumor grown in a wild-type (*G*) or in a uPA deficient mouse (*H*). *Arrows*, CD34-positive vessels. *A*, *B*, *E*, *F*, *G*, and *H* are *bright-field* and *C* and *D* are *dark-field* micrographs. Scale bar: 100 μm (*A*, *B*, *C*, *D*, and *E*); 50 μm (*F*, *G*, and *H*).

reached a mean size of 2000 mm^3 50 days after cell inoculation (Fig. 3*A*). In contrast, tumors grown in uPA$^{-/-}$ mice had a significantly slower growth rate reaching a mean size of 1200 mm^3 50 days after cell inoculation ($P = 0.007$). The growth curves shown in Fig. 3*A* included 20 uPA$^{+/+}$ and 19 uPA$^{-/-}$ mice, and presents one experiment (experiment 3) representative of the three separate experiments performed.

We have recently reported a direct correlation between tumor size and plasma β-gal activity in mice carrying MDA-MB-435 BAG tumors (32). Thus, to confirm in a more objective manner the differences in the size of tumors growing in uPA$^{+/+}$ *versus* uPA$^{-/-}$ mice, plasma β-gal content of tumor-bearing mice was measured. Data from experiments 2 and 3 were combined. Whereas uPA$^{+/+}$ mice had a mean plasma β-gal activity of 35,000 (range, 276–178.000; $n = 24$) the mean β-gal activity measured in uPA$^{-/-}$ tumor bearing mice was significantly lower (9.230, Range 327–38.900; $n = 29$; $P = 0.006$), thus confirming the observed differences in tumor volume (Fig. *3B*).

Local Invasion and Metastasis Formation of MDA-MB-435 BAG Xenografts. Histological inspection of the tumors grown in uPA$^{+/+}$ or uPA$^{-/-}$ mice showed that the tumors grew locally invasive, infiltrating the peritoneal wall of the animals in both groups. Fig. *2*, *E* and *F*, show a representative area with invasion of MDA-MB-435 BAG cells into the peritoneal wall of a uPA$^{-/-}$ mouse.

Lungs from tumor-bearing animals in experiment 3 were removed at autopsy (day 52) and processed for X-gal staining. Eighteen of 20 lungs from wild-type mice were evaluable. Fourteen of 18 (78%) of uPA$^{+/+}$ mice had stereomicroscopically visible metastases (blue dots) on the surface of the lungs. In contrast, only 10 out 19 uPA$^{-/-}$ mice (53%) showed surface lung metastases. Fishers exact test showed that uPA$^{-/-}$ mice had a trend toward a reduced number of animals with lung metastases ($P = 0.2$). By counting the number of surface metastasis (blue dots) on individual lungs, the mean number of metas-

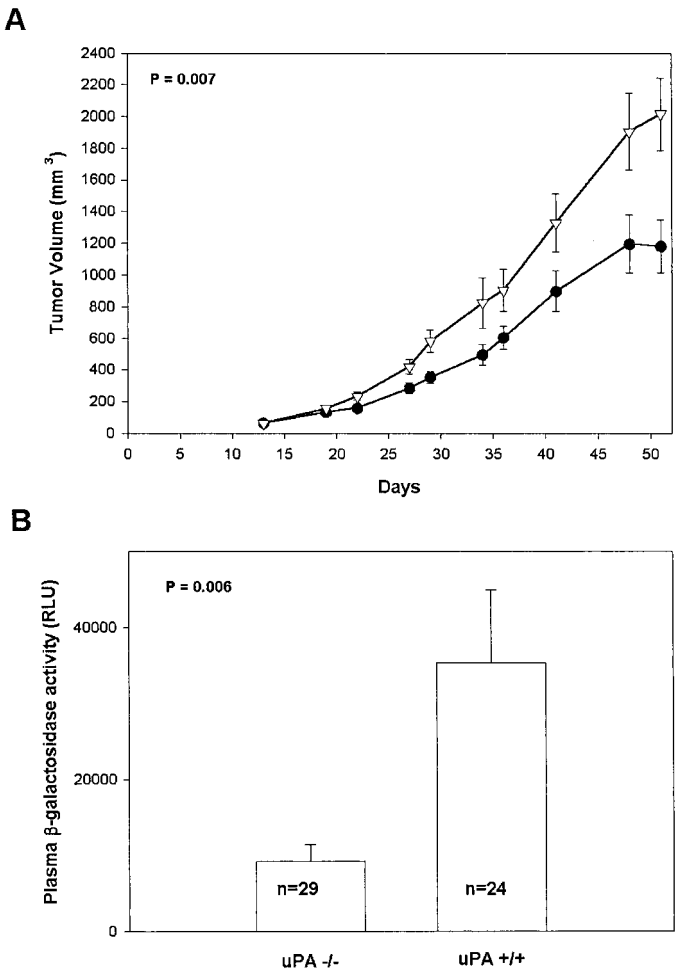

Fig. 3. Effect of uPA deficiency on primary tumor growth in mice inoculated s.c. with MDA-MB-435 BAG human breast cancer cells. *A*, plot of mean tumor volume *versus* time after inoculation of 2×10^6 cells/site/mouse. ●, *uPA*-deficient mice ($n = 19$); ○, wild-type mice ($n = 20$). The growth curves shown are representative of three separate experiments. *B*, plasma β-gal activity in mice carrying MDA-MB-435 BAG tumors. *Bars*, SE.

tases in $uPA^{+/+}$ mice was 12.7 (range, 0–36) whereas the mean number of surface lung metastases in $uPA^{-/-}$ was 4.7 (range, 0–80). By applying the Mann-Whitney nonparametric test, a trend appeared toward fewer lung surface metastases in $uPA^{-/-}$ mice ($P = 0.15$).

Thus, the difference between the groups regarding lung metastases did not reach statistical significance, but a tendency toward fewer metastases in the $uPA^{-/-}$ mice was evident.

CD34 Immunostaining of MDA-MB-435 BAG Tumors. Microscopic inspection of CD34-stained MDA-MB-435 BAG tumors from both $uPA^{+/+}$ and $uPA^{-/-}$ mice revealed positively stained vessels and capillaries throughout the tumor tissue (Fig. 2, *G* and *H*) and in the connective tissue surrounding the tumors.

No obvious differences appeared between the two groups, including no apparent differences in size or morphology.

Quantitation of Tumor Angiogenesis. In experiment 2, stereological evaluation of the number of CD34-immunostained capillaries (vascular profiles) showed a nonsignificant difference ($P = 0.15$) in vascular length density between $uPA^{-/-}$ mice ($n = 11$; 19 ± 4 profiles/mm^2) and $uPA^{+/+}$ mice ($n = 8$; one mouse was lost before termination of the experiment; 22 ± 4 profiles/mm^2). In addition to vascular length density, we examined at average maximal diffusion distance from capillary to tumor (0.13 mm $\pm$ 0.01 (SE) in $uPA^{-/-}$ mice and 0.12 mm $\pm$ 0.004 (SE) in $uPA^{+/+}$ mice) as well as total length of vessels in vital tumor tissue (8.5 m $\pm$ 1.7 (SE) in $uPA^{-/-}$ mice and 14.0 m $\pm$ 4.6 (SE) in $uPA^{+/+}$mice). In both cases we found the differences to be nonsignificant ($P = 0.16$ and $P = 0.23$, respectively), but with a trend toward reduced angiogenesis in tumors grown in the *uPA* gene-deficient mice. Thus, for all 3 types of measurements for tumor angiogenesis, we found a nonsignificant trend toward lower tumor angiogensis in the $uPA^{-/-}$ mice as compared with $uPA^{+/+}$ mice.

DISCUSSION

In the present study we used combined *uPA* gene-disrupted and immunodeficient mice as well as species-specific quantitation systems, which allowed us to investigate the importance of host stromal/cancer cell interactions with regard to uPA. The results obtained provide direct evidence of a tumor growth-promoting role of stromal cell produced uPA.

For the mRNA expression studies, the applied human- and mouse-specific uPA probes were clearly species-specific, and by including both murine and human uPA standard curves in the ELISA, we unequivocally demonstrated that this uPA ELISA does react with human, but not with murine, uPA. By the use of littermate animals as controls, we have attempted to minimize other host factors than uPA, influencing tumor growth and dissemination. Genotypes of the animals included in the experiments were in addition to PCR analyses, confirmed by subsequent murine uPA *in situ* hybridizations of the tumors.

We have described previously that mouse uPA is expressed in the human MDA-MB-231 breast cancer when grown in nude mice (3). Although using another human breast cancer cell line in the present study, the data confirm that the murine compartment of the human breast cancer xenografts express uPA. The murine uPA mRNA expression in MDA-MB-435 BAG tumors was confined to fibroblast-like cells, however, not all stromal cells with fibroblast-like appearance expressed murine uPA. Thus, the expression pattern of murine uPA in the xenografted human tumors resembles that described for human breast cancer (1).

The binding of uPA to its receptor strongly enhances cell-surface plasminogen activation (33). However, uPA binding to uPAR shows strict species specificity, *e.g.*, murine uPA does not bind human uPAR and *vice versa* (34). Thus, to fully exert its proteolytic potential, murine uPA must bind murine uPAR. In our previous study of MDA-MB-231 xenografts (3), murine uPA and uPAR were shown to be expressed by cells that were either the same or located very close to each other. Although we did not include analysis of murine uPAR in the present study, we assume that murine uPAR is also expressed in MDA-MB-435 BAG xenografts. Thus, coexpression of murine uPA and uPAR in the same or adjacent cells in the xenografted tumors makes it likely that the murine uPA system is involved in plasmin generation in the tumor tissue. The exact mechanisms regulating stromal cell uPA expression in tumors is unknown. *In vitro* studies have shown that a number of cytokines regulate uPA expression (35). In the xenografted tumors, the human cancer cells may be the source of cytokines, which, by a paracrine mechanism, induces uPA (and uPAR) expression in the surrounding stromal cells.

There is ample experimental evidence that uPA has importance for tumor cell growth, *e.g.*, it has been shown by different groups that uPA has a direct stimulative effect on tumor cell proliferation *in vitro* (11, 12). Inhibition of uPA activity (6, 7) or inhibition of uPA-uPAR interaction (36, 37), results in impaired growth of experimental tumors. However, of particular interest is that in a recent experimental *in vivo* study (36) using the MDA-MB-231 human xenograft implanted into immunodeficient mice, both human and murine uPA-uPAR antagonists showed significant inhibition of primary tumor growth, suggesting that both tumor- (human) and stromal- (murine) cell uPAR dependent plasminogen activation can modulate tumor growth *in vivo*.

Our experimental data are in agreement with the study of Tressler *et al.* (36). By genetic disruption of the *uPA* gene, we have shown that tumors grown in the gene-deleted animals have a significantly slower growth rate than tumors grown in littermate control animals. One explanation to the observed decreased growth rate of tumors in $uPA^{-/-}$ mice is that the local activation/release of growth factors is decreased attributable to decreased proteolytic activity in the tumor tissue (9, 10). Another explanation relates to the putative role of proteinases in the angiogenic process. Although the bioavailability of growth factors such as basic fibroblast growth factor, which is a highly efficient stimulator of angiogenesis, may be reduced in the tumor tissue of the $uPA^{-/-}$ mice, proteinases have also been ascribed a direct role in the migration of endothelial cells (review by Pepper *et al.* in Ref. 38). Endothelial cells express both uPA and uPAR (38, 39), and the interaction between these two molecules may govern endothelial cell migration in the extracellular matrix. In support of this notion is the demonstration of decreased angiogenesis in murine tumors exposed to a murine uPA-uPAR-inhibitor (37). In our study we found a nonsignificant trend toward a lower angiogenesis as measured by vascular density, total vascular length, as well as the maximal diffusion distance, in tumors in the $uPA^{-/-}$ mice.

Dissemination of cancer cells with subsequent formation of secondary tumors (metastasis), require proteinase activity and the ability to migrate and attach of not only the cancer cells but also of cells of the supporting stroma. A number of experimental tumor studies have shown that inhibition of uPA activity (4, 5) or uPA-uPAR interaction (40) results in a reduced number of metastatic foci. In our model, a difference although not significant was seen between $uPA^{+/+}$ and $uPA^{-/-}$ mice with regard to the number of lung surface metastases formed from the primary tumors, suggesting that stromal uPA is also involved in the mechanisms of metastasis formation. However, because of the significant effect of uPA-deficiency on the growth of the primary tumors, it cannot be excluded that the effect seen on the number of lung surface metastases reflects the effect on growth, *i.e.*, some of the metastases in the $uPA^{-/-}$ mice are under the detection limit of our evaluation system. In support of this notion is that tumors

showed an invasive growth pattern in both wild-type and uPA$^{-/-}$ mice.

In conclusion, the experimental data obtained points to a direct role of stromal-derived uPA for the growth of the human MDA-MB-435 BAG breast cancer xenograft.

REFERENCES

1. Nielsen, B. S., Sehested, M., Timshel, S., Pyke, C., and Danø, K. Messenger RNA for urokinase plasminogen activator is expressed in myofibroblasts adjacent to cancer cells in human breast cancer. Lab. Investig., *74:* 168–177, 1996.
2. Pyke, C., Græm, N., Ralfkiær, E., Rønne, E., Høyer-Hansen, G., Brünner, N., and Danø, K. Receptor for urokinase is present in tumor-associated macrophages in ductal breast carcinoma. Cancer Res., *53:* 1911–1915, 1993.
3. Rømer, J., Pyke, C., Lund, L. R., Eriksen, J., Kristensen, P., Rønne, E., Høyer-Hansen, G., Danø, K., and Brünner, N. Expression of uPA and its receptor by both neoplastic and stromal cells during xenograft invasion. Int. J. Cancer, *57:* 553–560, 1994.
4. Ossowski, L., and Reich, E. Antibodies to plasminogen activator inhibit human tumor metastasis. Cell, *35:* 611–619, 1983.
5. Mignatti, P., Robbins, E., and Rifkin, D. B. Tumor invasion through the human amniotic membrane: requirement for a proteinase cascade. Cell, *47:* 487–498, 1986.
6. Ossowski, L., Russo Payne, H., and Wilson, E. L. Inhibition of urokinase-type plasminogen activator by antibodies: the effect on dissemination of a human tumor in the nude mouse. Cancer Res., *51:* 274–281, 1991.
7. Wilhelm, O., Schmitt, M., Hohl, S., Senekowitsch, R., and Graeff, H. Antisense inhibition of urokinase reduces spread of human ovarian cancer in mice. Clin. Exp. Metastasis, *13:* 296–302, 1995.
8. Holst-Hansen, C., Johannessen, B., Høyer-Hansen, G., Rømer, J., Ellis, V., and Brünner, N. Urokinase-type plasminogen activation in three human breast cancer cell lines correlates with their *in vitro* invasiveness. Clin. Exp. Metastasis, *14:* 297–307, 1996.
9. Odekon, L. E., Blasi, F., and Rifkin, D. B. Requirement for receptor-bound urokinase in plasmin-dependent cellular conversion of latent TGF-β to TGF-β. J. Cell. Physiol., *158:* 398–407, 1994.
10. Ribatti, D., Leali, D., Vacca, A., Giuliani, R., Gualandris, A., Roncali, L., Nolli, M. L., and Presta, M. *In vivo* angiogenic activity of urokinase: role of endogenous fibroblast growth factor-2. J. Cell Sci., *112:* 4213–4221, 1999.
11. Kirchheimer, J. C., Wojta, J., Christ, G., Hienert, G., and Binder, B. R. Mitogenic effect of urokinase on malignant and unaffected adjacent human renal cells. Carcinogenesis (Lond.), *9:* 2121–2123, 1988.
12. De Petro, G., Copeta, A., and Barlati, S. Urokinase-type and tissue-type plasminogen activators as growth factors of human fibroblasts. Exp. Cell Res., *213:* 286–294, 1994.
13. Grøndahl-Hansen, J., Lund, L. R., Ralfkiær, E., Ottevanger, V., and Danø, K. Urokinase- and tissue-type plasminogen activators in keratinocytes during wound repepithelialization. J. Investig. Dermatol., *90:* 790–795, 1988.
14. Kramer, M. D., Schaefer, B., and Reinartz, J. Plasminogen activation by human keratinocytes: Molecular pathways and cell-biological consequences. Bio. Chem. Hoppe Seyler, *376:* 131–141, 1995.
15. Jensen, P. J., and Lavker, R. M. Urokinase is a positive regulator of epidermal proliferation *in vivo*. J. Investig. Dermatol., *112:* 240–244, 1999.
16. Poliakov, A. A., Mukhina, S. A., Traktouev, D. O., Bibilashvily, R. S., Gursky, Y. G., Minashkin, M. M., Stepanova, V. V., and Tkachuk, V. A. Chemotactic effect of urokinase plasminogen activator: a major role for mechanisms independent of its proteolytic or growth factor domains. J. Recept. Signal Transduct. Res., *19:* 939–951, 1999.
17. Carmeliet, P., Schoonjans, L., Kieckens, L., Ream, B., Degen, J., Bronson, R., De Vos, R., van den Oord, J. J., Collen, D., and Mulligan, R. C. Physiological consequences of loss of plasminogen activator gene function in mice. Nature (Lond.), *368:* 419–424, 1994.
18. Carmeliet, P., Moons, L., Herbert, J. M., Crawley, J., Lupu, F., Lijnen, R., and Collen, D. Urokinase but not tissue plasminogen activator mediates arterial neointima formation in mice. Circ. Res., *81:* 829–839, 1997.
19. Lijnen, H. R., Van Hoef, B., Lupu, F., Moons, L., Carmeliet, P., and Collen, D. Function of the plasminogen/plasmin and matrix metalloproteinase systems after vascular injury in mice with targeted inactivation of fibrinolytic system genes. Arterioscler. Thromb. Vasc. Biol., *18:* 1035–1045, 1998.
20. Lijnen, H. R., Lupu, F., Moons, L., Carmeliet, P., Goulding, D., and Collen, D. Temporal and topographic matrix metalloproteinase expression after vascular injury in mice. Thromb. Haemost., *81:* 799–807, 1999.
21. Bugge, T. H., Flick, M. J., Danton, M. J. S., Daugherty, C. C., Rømer, J., Danø, K., Carmeliet, P., Collen, D., and Degen, J. L. Urokinase-type plasminogen activator is effective in fibrin clearance in the absence of its receptor or tissue-type plasminogen activator. Proc. Nat. Acad. Sciences USA, *93:* 5899–5904, 1996.
22. Shapiro, R. L., Duquette, J. G., Roses, D. F., Nunes, I., Harris, M. N., Kamino, H., Wilson, E. L., and Rifkin, D. B. Induction of primary cutaneous melanocytic neoplasms in urokinase-type plasminogen activator (uPA)-deficient and wild-type mice-cellular blue nevi invade but do not progress to malignant melanoma in uPA-deficient animals. Cancer Res., *56:* 3597–3604, 1996.
23. Brünner, N., Thompson, E. W., Spang-Thomsen, M., Rygaard, J., Danø, K., and Zwiebel, J. A. lacZ transduced human breast cancer xenografts as an *in vivo* model for the study of invasion and metastasis. Eur. J. Cancer, *28A:* 1989–1995, 1992.
24. Kristensen, P., Eriksen, J., Blasi, F., and Danø, K. Two alternatively spliced mouse urokinase receptor mRNAs with different histological localization in the gastrointestinal tract. J. Cell Biol., *115:* 1763–1771, 1991.
25. Camiolo, S. M., Siuta, M. R., and Madeja, J. M. Improved medium for extraction of plasminogen activator from tissue. Prep. Biochem. Biotechnol., *12:* 297–305, 1982.
26. Benraad, T. J., Geurtsmoespot, J., Grøndahl-Hansen, J., Schmitt, M., Heuvel, J. J. T. M., Dewitte, J. H., Foekens, J. A., Leake, R. E., Brünner, N., and Sweep, C. G. J. Immunoassays (ELISA) of urokinase-type plasminogen activator (uPA): report of an EORTC/BIOMED-1 workshop. Eur. J. Cancer, *32A:* 1371–1381, 1996.
27. Pyke, C., Kristensen, P., Ralfkiær, E., Grøndahl-Hansen, J., Eriksen, J., Blasi, F., and Danø, K. Urokinase-type plasminogen activator is expressed in stromal cells and its receptor in cancer cells at invasive foci in human colon adenocarcinomas. Am. J. Pathol., *138:* 1059–1067, 1991.
28. Ponte, P., Ng, S. Y., Engel, J., Gunning, P., and Kedes, L. Evolutionary conservation in the untranslated regions of actin mRNAs: DNA sequence of a human β-actin cDNA. Nucleic Acids Res., *12:* 1687–1696, 1984.
29. Feinberg, A. P., and Vogelstein, B. A technique for radiolabeling DNA restriction endonuclease fragments to high specific activity. Anal. Biochem., *132:* 6–13, 1983.
30. Holst-Hansen, C., Brünner, N., Johannessen, B. E., Felding, J., and Stephens, R. W. A new immunocapture assay for *Escherichia coli* β-galactosidase for *in vivo* studies of lacZ-transduced tumor cells. Lab. Investig., *78:* 1643–1644, 1998.
31. Gundersen, H. J., Bendtsen, T. F., Korbo, L., Marcussen, N., Møller, A., Nielsen, K., Nyengaard, J. R., Pakkenberg, B., Sørensen, F. B., and Vesterby, A. Some new, simple and efficient stereological methods and their use in pathological research and diagnosis. APMIS, *96:* 379–394, 1988.
32. Holst-Hansen, C., Stephens, R. W., Johannessen, B. E., Jensen, P. B., and Brünner, N. Plasma *Escherichia coli* β-galactosidase as a marker of tumor burden and response to experimental anti-neoplastic therapy in nude mice xenografted with lacZ transduced human tumor cells. Lab Investig., *80:* 719–724, 2000.
33. Ellis, V., Behrendt, N., and Danø, K. Plasminogen activation by receptor-bound urokinase. A kinetic study with both cell-associated and isolated receptor. J. Biol. Chem., *266:* 12752–12758, 1991.
34. Solberg, H., Rømer, J., Brünner, N., Holm, A., Sidenius, N., Danø, K., and Høyer-Hansen, G. A cleaved form of the receptor for urokinase-type plasminogen activator in invasive transplanted human and murine tumors. Int. J. Cancer, *58:* 877–881, 1994.
35. Bechtel, M. J., Reinartz, J., Rox, J. M., Inndorf, S., Schaefer, B. M., and Kramer, M. D. Upregulation of cell-surface-associated plasminogen activation in cultured keratinocytes by interleukin-1-β and tumor necrosis factor-α. Exp. Cell Res., *223:* 395–404, 1996.
36. Tressler, R. J., Pitot, P. A., Stratton, J. R., Forrest, L. D., Zhuo, S., Drummond, R. J., Fong, S., Doyle, M. V., Doyle, L. V., Min, H. Y., and Rosenberg, S. Urokinase receptor antagonists: discovery and application to *in vivo* models of tumor growth. APMIS, *107:* 168–173, 1999.
37. Min, H. Y., Doyle, L. V., Vitt, C. R., Zandonella, C. L., Strattonthomas, J. R., Shuman, M. A., and Rosenberg, S. Urokinase receptor antagonists inhibit angiogenesis and primary tumor growth in syngeneic mice. Cancer Res., *56:* 2428–2433, 1996.
38. Pepper, M. S., Sappino, A. P., Stocklin, R., Montesano, R., Orci, L., and Vassalli, J. D. Upregulation of urokinase receptor expression on migrating endothelial cells. J. Cell Biol., *122:* 673–684, 1993.
39. Pepper, M. S., Vassalli, J. D., Montesano, R., and Orci, L. Urokinase-type plasminogen activator is induced in migrating capillary endothelial cells. J. Cell Biol., *105:* 2535–2541, 1987.
40. Li, H., Lu, H., Griscelli, F., Opolon, P., Sun, L. Q., Ragot, T., Legrand, Y., Belin, D., Soria, J., Soria, C., Perricaudet, M., and Yeh, P. Adenovirus-mediated delivery of a uPA/uPAR antagonist suppresses angiogenesis-dependent tumor growth and dissemination in mice. Gene Ther., *5:* 1105–1113, 1998.

[CANCER RESEARCH 62, 329–330, January 1, 2002]

Announcements

(Requests for announcements must be received at least three months before publication.)

FUTURE ANNUAL MEETINGS OF THE AMERICAN ASSOCIATION FOR CANCER RESEARCH

2002 April 6–10, San Francisco, CA
2003 April 5–9, Toronto, Ontario, Canada
2004 March 27–31, Orlando, FL

AACR SPECIAL CONFERENCES IN CANCER RESEARCH

A number of meetings are now being organized in the AACR's series of smaller scientific meetings. Following are the topics, dates, locations, and program committees for these meetings. When full details of each meeting are available, AACR members will be the first to receive complete brochures and application forms for participation in these important conferences. Nonmembers may receive this information by sending their names and addresses to Meetings Mailing List, American Association for Cancer Research, Public Ledger Building, 150 South Independence Mall West, Suite 826, Philadelphia, PA 19106-3483. Up-to-date program information is also available via the Internet at the AACR's website (http://www.aacr.org).

MOLECULAR IMAGING IN CANCER: LINKING BIOLOGY, FUNCTION, AND CLINICAL APPLICATIONS IN VIVO

January 23–27, 2002
Disney's Contemporary Resort, Lake Buena Vista, FL

Chairpersons
David Piwnica-Worms, St. Louis, MO
Thomas J. Meade, Pasadena, CA
Patricia M. Price, Manchester, England

APOPTOSIS AND CANCER: BASIC MECHANISMS AND THERAPEUTIC OPPORTUNITIES IN THE POST-GENOMIC ERA

February 13–17, 2002
Hilton Waikoloa Resort, Waikoloa, Hawaii

Chairpersons
John C. Reed, La Jolla, CA
Scott W. Lowe, Cold Spring Harbor, NY

THE MOLECULAR GENETICS OF COLON CANCER

March 7–10, 2002
Loew's Philadelphia Hotel, Philadelphia, PA

Chairpersons
Anil K. Rustgi, Philadelphia, PA
Raju Kucherlapati, Bronx, NY

ONCOGENOMICS 2002: DISSECTING CANCER THROUGH GENOME RESEARCH

May 1–5, 2002
Burlington Hotel, Dublin, Ireland

Chairpersons
Jeffrey M. Trent, Bethesda, MD
Bette Phimister, New York, NY

CALENDAR OF EVENTS

Fourth International Symposium on Anti-Angiogenic Agents: Recent Advances and Future Directions in Cell Biology and Clinical Research, January 10–13, 2002, Adam's Mark Hotel, Dallas, TX. Contact: Kim Pearson, The CBCE, 8445 Freeport Parkway, Suite 680, Irving, TX 75063. Phone: 972.929.1900 (x104); Fax: 972.929.1901; E-mail: symposia@theCBCE.com.

13th Annual Colorectal Disease Symposium: An International Exchange of Medical and Surgical Concepts, February 14–16, 2002, Marriot's Harbor Beach Resort and Spa, Fort Lauderdale, FL. 25.5 Category I CME credit hours. Contact: Cleveland Clinic Florida, Department of Continuing Education, 2950 Cleveland Clinic Boulevard, Weston, FL 33331. Phone: 954.659.5490; Fax: 954.659.5491; E-mail: cme@ccf.org; Website: www.cmeccf.com.

7th Annual NCCN Conference: Practice Guidelines and Outcomes Data in Oncology, February 28–March 3, 2002, Westin Diplomat Resort and Spa, Hollywood, FL. Contact: Tricia Wilson, National Comprehensive Cancer Network, 50 Huntingdon Pike, Suite 200, Rockledge, PA 19046. Phone: 215.728.2577; Fax: 215.728.3877; E-mail: information@nccn.org; Website: www.nccn.org.

International Symposium on Antimutagenesis and Anticarcinogenesis, April 26, 2002, New York Medical College, Valhalla, New York. Contact: Kathy Woodley, Basic Science Building, New York Medical College, Valhalla, NY 10595. Phone: 914.594.3084; Fax: 914.594.4163; E-mail: Kathy_Woodley@nymc.edu.

Molecular, Biologic, and Genetic Mechanisms Underlying Molecular Cancer: Implication of Early Detection, Screening, and Prevention, May 6–7, 2002, Magee Womens Hospital, Main Auditorium, Pittsburgh, PA. Contact: Lori Burleigh, Women's Health Program, University of Pittsburgh, PA 15260. Phone: 412-624-3045; Fax: 412-624-1056.

15th International Symposium of the Journal of Steroid Biochemistry and Molecular Biology: Recent Advances in Steroid Biochemistry and Molecular Biology, May 17–20, 2002, Munich, Germany. Contact: Prof. J. R. Pasqualini, Institut de Puériculture, 26 Boulevard Brune, 75014 Paris, France. Phone: 33-1.45.39.91.09; Fax: 33-1.45.42.61.21; E-mail: Jorge.Pasqualini@wanadoo.fr.

17th Annual Offering of Critical Issues in Tumor Microcirculation, Angiogenesis, and Metastasis: Biological Significance and Clinical Relevance: A Continuing Education Course of Harvard Medical School and Massachusetts General Hospital, June 3–6, 2002, Boston, MA. 22 credit hours in category I of the Physician's Recognition Award of the American Medical Association. Website: http://steele.mgh.harvard.edu.

7th International Symposium on Dendritic Cells, September 19–24, 2002, Bamberg, Germany. For more information go to http://www.dc2002.de.

First Annual Scientific Meeting of the International Society for the Prevention of Tobacco Induced Diseases (PTID Society); Centuries of Tobacco Caused Diseases and Mortality, October 28–30, 2002, Essen, Germany. For more information see the web: www.ptid2002.info or contact per fax: +49 (40) 360.395.9983 or e-mail: TOXICOL98@AOL.COM.

18th World Congress of Digestive Surgery and 9th Hong Kong International Cancer Congress, December 8–11, 2002, Hong Kong Convention and Exhibition Centre, Wanchai, Hong Kong. Contact: Congress Secretariat, 18th World Congress of Digestive Surgery (WCDS2002), Department of Surgery, University of Hong Kong Medical Centre, Queen Mary Hospital, Hong Kong. Phone: 852.2818.0232/852.2855.4235; Fax: 852.2818.1186; E-mail: wcds2002@hkucc.hku.hk; Website: http://www.wcds2002.org.

Corrections

In the article by J. A. Loncaster *et al*., entitled "Carbonic Anhydrase (CA IX) Expression, a Potential New Intrinsic Marker of Hypoxia: Correlations with Tumor Oxygen Measurements and Prognosis in Locally Advanced Carcinoma of the Cervix," which appeared in the September 1, 2001 issue of *Cancer Research* (pp. 6394–6399), the sixth author's name appeared incorrectly as Charles C. **Wycoff**. The author's correct name is Charles C. **Wykoff**.

Charles C. Wykoff

In the article by T. L. Frandsen *et al*., entitled "Direct Evidence of the Importance of Stromal Urokinase Plasminogen Activator (uPA) in the Growth of an Experimental Human Breast Cancer Using a Combined *uPA* Gene-Disrupted and Immunodeficient Xenograft Model," which appeared in the January 15, 2001 issue of *Cancer Research* (pp. 532–537), the equation on page 534 appeared incorrectly as:

$$L_v(\text{vasc/tumor}) = \frac{Q_A(\text{vasc})}{\{2 \cdot 2 \cdot \Sigma P(\text{tumor})\}}$$

The correct equation appears below.

$$L_V(\text{vasc/tumor}) = 2 \cdot Q_A(\text{vasc})/[(a/p) \cdot \Sigma P(\text{tumor})]$$

Thomas Leth Frandsen
Claus Holst-Hansen
Boye Schnack Nielsen
Ib Jarle Christensen
Jens R. Nyengaard
Peter Carmeliet
Nils Brünner

Erratum

In the correspondence from B. Pasche *et al*., entitled "*TβR-1(6A)* Association with Colorectal Cancer: A New Twist," which appeared in the November 15, 2001 issue of *Cancer Research* (pp. 8351–8352), the second sentence appeared incorrectly as, "Eighteen of these patients were *TβR-I(6A)* **homozygotes**." The correct sentence is, "Eighteen of these patients were *TβR-I(6A)* **heterozygotes**."

Direct Evidence of the Importance of Stromal Urokinase Plasminogen Activator (uPA) in the Growth of an Experimental Human Breast Cancer Using a Combined *uPA* Gene-Disrupted and Immunodeficient Xenograft Model

Thomas Leth Frandsen, Claus Holst-Hansen, Boye Schnack Nielsen, et al.

Cancer Res 2001;61:532-537.